DETAILED ANALYSIS OF ANNEALING SILVER FRONT SIDE CONTACTS ON SILICON SOLAR CELLS

S. Kontermann, A. Grohe, R. Preu
Fraunhofer Institute for Solar Energy Systems (ISE)
Heidenhofstrasse 2, 79110 Freiburg, Germany
Telephone: 49 761 4588 5435, Facsimile: +49 761 4588 9250
E-mail: stefan.kontermann@ise.fraunhofer.de

ABSTRACT

New concepts for high efficient solar cells require a post processing annealing step for passivation quality improvement. For cutting costs, thick film metallization is used for the front side. In this paper annealing steps of different duration and temperature are applied to standard industrial silicon solar cells to probe the sensitivity for such a front side metallization towards annealing. This paper focuses on five minute annealing under nitrogen atmosphere and determines favourable annealing temperatures and metallization pastes. In our investigations I-V curve measurements showed that from a certain threshold onwards, an increasing thermal budget decreases cell's performance. Series and contact resistance measurements were determined to be significantly affected by annealing. Scanning electron microscopy (SEM) revealed that silver crystallites at the silver silicon interface are transformed in shape for annealing at high temperatures which is most probable the microscopic reason for an increased contact resistance.

INTRODUCTION

So far annealing has been investigated on silicon solar cells with thick film metallization for a temperature range where annealing is mostly beneficial. Research analysed annealing steps incorporated in the firing process, i.e. without cooling down the wafer to room temperature after firing [1] while a stand alone forming gas annealing step was investigated in [2].
One concept of the next cell type being transferred to industrial production incorporates a standard front side metallization with screen printed silver thick film contacts and a passivated rear side with local contacts [3]. While this cell type requires an annealing step for exhibiting the advantage of improved rear side passivation, annealing might be inferior to the front side metallisation, depending on the annealing conditions. As for this type of rear side high temperatures are favourable, it is a requirement on the front side metallization to support this temperature. We pushed annealing temperatures so far that cells experienced a loss in fill factor in order to determine what temperature is still acceptable for the front side contact.

EXPERIMENTAL

Solar Cell Fabrication

Standard industrial Al-BSF silicon solar cells were fabricated on 156×156 mm² mc silicon wafers of 240 µm thickness, p-type, 0.5 - 2.0 Ωcm. Processing included wet chemical etching for texturing, $POCl_3$ emitter diffusion, silicon nitride antireflection coating and screen printing back and front side contacts. In total we used six different metal pastes for the front side metallization. Firing was done in a belt furnace where peak firing temperatures was varied in steps of 20 K around the optimum peak firing temperature for each paste. The finished solar cells were cut into pieces of 50 x 40 mm² to provide more samples.

Annealing

Annealing was accomplished in an optically heated belt furnace. For obtaining significant results, wafer temperatures need to be properly held at the set annealing temperature and time. To account for this, temperature profiles were measured. A wafer equipped with several thermocouples across was run through the furnace while a data acquisition device was recording the temperature. Temperature controls for the heating zones of the furnace and the belt speed have been adjusted until a smooth profile for the cell's temperature and the correct annealing time were achieved. Temperature profiles for all annealing experiments were established in this manner.
Figure 1 displays the optimised profiles obtained from the described method at desired plateau temperatures of 250 °C, 390 °C and 510 °C and 5 minutes duration. Heating and cooling rates were 7 K/s and 1.5°K/s respectively. In figure 1, each thermocouple on the test cell shows equal temperatures with time, meaning that the temperature distribution across the cell was uniform and the cell was heated homogenously. The temperature on the plateau stayed within a deviation from the desired temperature of $\Delta T < 10$ K for all times.

978-1-4244-1641-7/08/$25.00 ©2008 IEEE

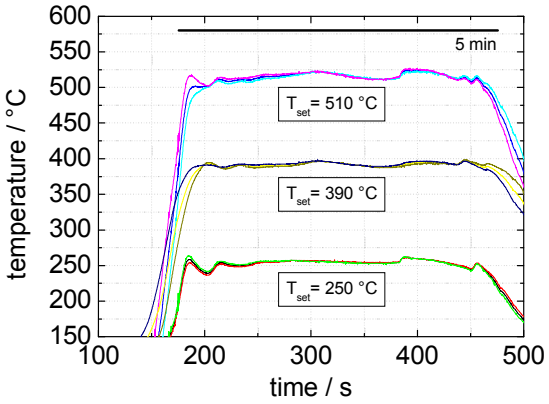

Fig. 1 Optimised annealing temperature profiles measured with thermocouples

For annealing we selected from each paste those cells that were fired at optimum peak firing temperature and yielded a high fill factor of FF > 77 %. This ensured investigations to be on a high performance level. The cells were annealed under nitrogen atmosphere at temperatures between 250 °C and 570 °C for 5 minutes according to the measured profiles. Duration was chosen to be 5 minutes, as a short annealing time showed to provide better results [4].

Results IV parameters

IV-curves were measured for all cells before and after annealing. Figures 2a and 2b display the relative change in IV-curve parameters in dependence of the annealing temperature for two pastes. The fill factor of paste 3 is enhanced for annealing up to a temperature of 570 °C. This is remarkable, as 570 °C is very close to the Al-Si eutectic temperature of 577 °C. Paste 3 was intentionally designed for use on mc silicon wafers. That explains the better performance in this case.

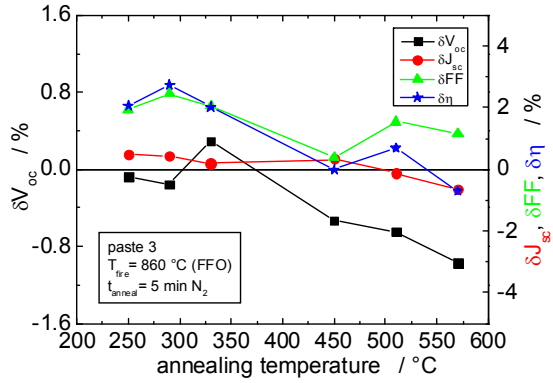

Fig. 2a: Relative deviation of IV parameters before and after annealing at different temperatures, paste 3

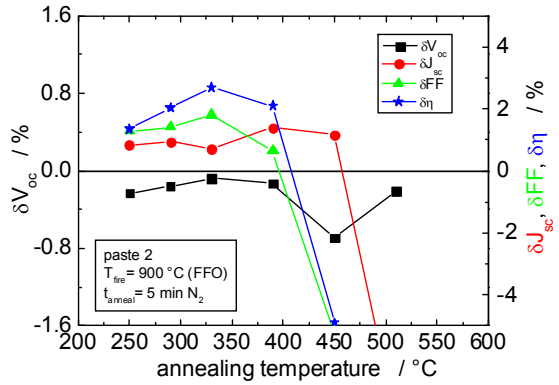

Fig. 2b: Relative deviation of IV parameters before and after annealing at different temperatures, paste 2

For paste 2 the fill factor is increased up to a temperature of 390 °C. Above this temperature the fill factor decreases significantly.
For both pastes the short circuit current is enhanced by 0.3 % except for temperatures above 510 °C, while the open circuit voltage is decreased at the most by 0.9 %.

Contact resistance measurements

$1.5 \times 4\ cm^2$ pieces were cut from the fabricated cells with a dicing saw for measuring contact resistances according to the transmission line method (TLM) [5,6].
Measurements of the contact resistance R_C and the specific contact resistance ρ_C by TLM as well as calculations of the series resistance under illumination R_{s_light} according to [7] were performed. Results are displayed in figures 3a and 3b..

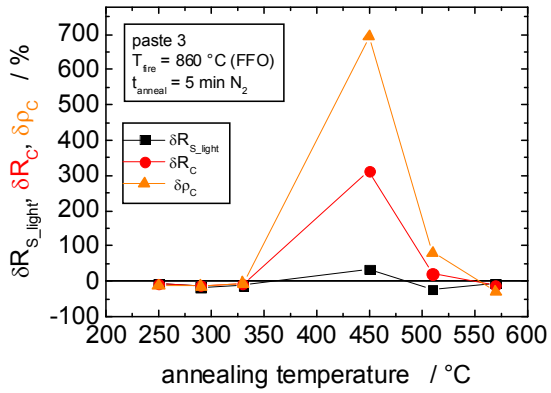

Fig. 3a: relative deviation of R_{S_light}, R_C and ρ_C before and after annealing for the cells from Fig. 2a

978-1-4244-1641-7/08/$25.00 ©2008 IEEE

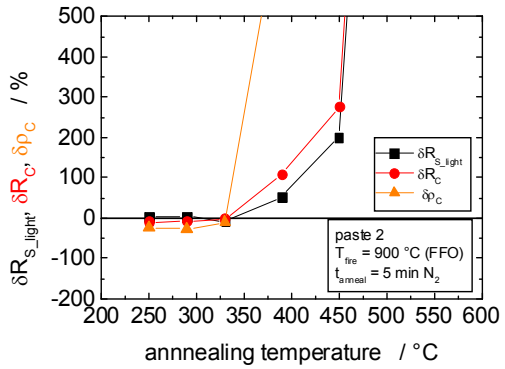

Fig. 3b: relative deviation of R_{S_light}, R_C and ρ_C before and after annealing for the cells from Fig. 2b

The curves reveal that the specific contact resistance ρ_C and the series resistance R_{S_light} show qualitatively the same development. From this we deduct that it is mainly the contact resistance that influences the series resistance. The development of the curves for the series resistances shows that the fill factor is ruled by: R_{S_light}, as they show anti-proportional behaviour. Thus the significant parameter is the contact resistance. To gain mor insight into this, we chose to analyze the contact interface by SEM.

SEM investigation

For SEM investigations, 3 pieces of 10 × 10 mm^2 of each of the solar cells were prepared. The first sample was used for imaging the finger surface. The second was cut half through in thickness, dipped in liquid nitrogen and cracked just before inserting into the SEM for cross section investigations. The third sample was used to obtain access to the contact interface. These pieces were chemically etched several times in different acids to remove the front side contact. For process details see [8].

Figures 4a-c show the SEM images. Images on the left were taken before annealing from a sample with a fill factor of FF = 77.8 %. Images on the right from a sample that was annealed for 5 minutes at 510°C under nitrogen resulting in a fill factor decrease from FF >77 % down to FF = 66.4 %.

Figure 4a shows that annealing affects the surface of the silver bulk, as pimples arose after annealing. This might have affected the conductivity of the finger and thus increased the series resistance. Figure 4b reveals that silver crystallites [1,8-11] at the interface between the silver finger and the silicon bulk have the shape of a pyramid before annealing but tend to be lenticular after annealing. This is confirmed by the SEM images in figures 4c and 4d where the imprints of the pyramid on the silicon surface are shown. Before annealing the inverted pyramids originating from the silver crystals have straight edges while those after annealing are curved.

This effect has been observed as well for over-fired samples [4]. As the SEM samples were all cut from the same cell that was fired at optimum PFT, it is very unlikely that this cell was over-fired and that the curved imprints thus originate from this fact. Nevertheless, it might be possible that over-firing occurred due to temperature inhomogenities from belt shading during firing as discussed in [8]. But even this is unlikely as the cell had a very good fill factor of FF = 77.8 % after firing. From this we deduce that annealing at temperatures where fill factors decrease significantly, the crystals and the microstructure of the Ag/Si interface is affected. A decreasing fill factor goes along with an increasing series resistance predominantly by an increased contact resistance.

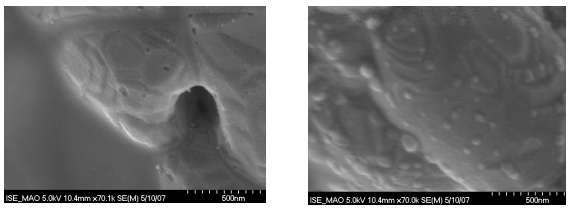

Fig. 4a: SEM top view on front contact fingers of a sample before (left), and after annealing (right)

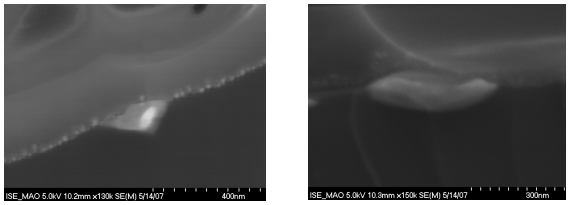

Fig. 4b: SEM cross section of Ag-Si interface of the samples from figure 4a

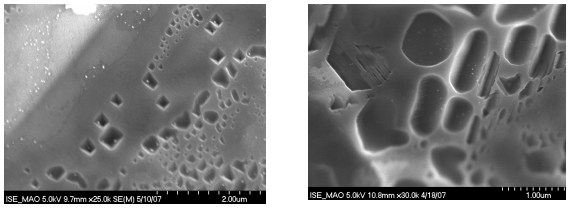

Fig. 4c: SEM top view after contact removal of the samples from figure 4a

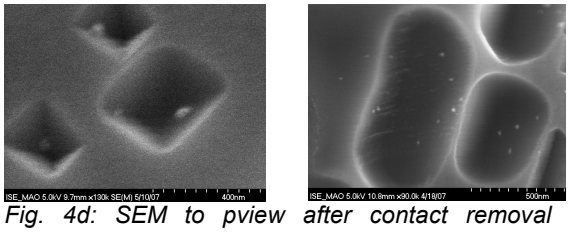

Fig. 4d: SEM to pview after contact removal samples from 4c (enlarged)

978-1-4244-1641-7/08/$25.00 ©2008 IEEE

The process of crystal deforming is most likely to happen during annealing. The only other possibility is that this occurs due to Ag diffusion into the silicon below the Ag/Si interface resulting in an increased etching rate during the contact lift-off compared to the etch rate of pure silicon.
The increased contact resistance might originate from the glass frit separating the crystals from the silver finger. After firing, this layer of glass frit is located already disadvantageously between the silver fingers and the crystals. But the frit layer is locally penetrated and crystals make contact to the silver bulk. During annealing it is possible that the glass frit is softened below its melting point and is able to redistribute more homogeneously and thus isolating more crystals. This would results in a higher contact resistance that we observed with the TLM measurements.

CONCLUSIONS/Summary

This paper analyses the impact of different annealing steps on the IV curve and the contact microstructure of mc silicon solar cells. Cell performance after annealing is strongly dependent on annealing temperature and the metal paste used for metallization. For temperatures up to 390 °C all pastes showed a beneficial effect on fill factor and efficiency. Only one paste allowed for annealing up to 510 C without performance loss. Contact resistance measurements according to the transmission line method show that annealing affects the contact resistance depending on temperature and paste. For temperatgures below 390 °C contact resistance is decreased for all contacts under test. SEM investigations on the microstructure of the silver silicon interface reveal that annealing affects the shape of the silver crystals at the Ag/Si interface. This is a possible mechanism that alters the contact resistances.

Acknowledgement

The authors would like to thank E. Schäffer for IV curve measurements. S. Kontermann is financially supported by the scholarship program of the Stiftung der Deutschen Wirtschaft (*sdw*) and a scholarship of the Albert-Ludwigs-University of Freiburg, Germany. This work was supported by the German Federal Ministry for the Environment, Nature Conservation and Reactor Safety (BMU) under project no. 0327572.

REFERENCES

[1] G. Grupp et al., *20th EU PVSEC*, 2005, Barcelona, Spain.

[2] G. Schubert et al., 2*1st EU PVSEC*, 2006, Dresden, Germany

[3] E. Schneiderlöchner et al., ”Status and Advancement in Transferring the Laser-Fired Contact Technology to Screen-Printed Silicon Solar Cells”, *20th EU PVSEC*, 2005,. Barcelona, Spain.

[4] S. Kontermann et al., ”Investigations on the Influence of Different Annealing Steps on Silicon Solar Cells With Silver Thick Film Contacts”, *22nd EU PVSEC*, 2007. Milan, Italy.

[5] H.H. Berger, “Contact Resistance on Diffused Resistors”, *IEEE International Solid State Circuits Conference*. 1969.

[6] G.K. Reeves, H.B. Harrison, “Obtaining the Specific Contact Resistance from Transmission Line Model Measurements”, *IEEE Electron Device Letters*, 1982. **EDL-3**(5): p. 111-3.

[7] A. G. Aberle, S.R. Wenham and M.A. Green, “A New Method for Accurate Measurements of the Lumped Series Resistance of Solar Cells”, *23rd IEEE PVSC*, 1993. Louisville, Kentucky, USA.

[8] S. Kontermann et al., “Characterisation of Ssilver Thick Film Contact Formation on Textured Monocrystalline Silicon Solar Cells”, *21st EU PVSEC*, 2006, Dresden, Germany.

[9] G. Grupp et al., “Analysis of Silver Thick-Film Contact Formation on Industrial Silicon Solar Cells”, *31st IEEE PVSC*, 2005. Orlando, Florida, USA.

[10] D.M. Huljic et al., “Microstructural Analyses of Ag Thick-Film Contacts on n-type Silicon Emitters”, *3rd WCPEC*, 2003. Osaka, Japan.

[11] G. Schubert et al., “Current Transport Mechanism in Printed Ag Thick Film Contacts to an n-type Emitter of a Crystalline Silicon Solar Cell”, *19th EU PVSEC*, 2004,Paris, France.

978-1-4244-1641-7/08/$25.00 ©2008 IEEE